Characterization of *Mollivirus kamchatka*, the first modern representative of the proposed *Molliviridae* family of giant viruses.

Running title: characterization of the first modern mollivirus

Eugene Christo-Foroux[#a], Jean-Marie Alempic[a], Audrey Lartigue[a], Sebastien Santini[a], Matthieu Legendre[a] , Chantal Abergel[a] , Jean-Michel Claverie[#a]

a Aix Marseille Univ., CNRS, IGS, Information Génomique & Structurale (UMR7256), Institut de Microbiologie de la Méditerranée (FR 3489), Marseille, France

Correspondance to : Eugene.christo-foroux@igs.cnrs-mrs.fr, jean-michel.claverie@univ-amu.fr

Keywords: Paleovirology; Kamchatka; Comparative Genomics; Nucleo-cytoplasmic Large DNA viruses; Genome Structure.

Abstract

Microbes trapped in permanently frozen paleosoils (permafrost) are the focus of increasing researches in the context of global warming. Our previous investigations led to the discovery and reactivation of two Acanthamoeba-infecting giant viruses, *Mollivirus sibericum* and P*ithovirus sibericum* from a 30,000-year old permafrost layer. While several modern pithovirus strains have since been isolated, no contemporary mollivirus relative was found. We now describe *Mollivirus kamchatka*, a close relative to *M. sibericum*, isolated from surface soil sampled on the bank of the Kronotsky river in Kamchatka. This discovery confirms that molliviruses have not gone extinct and is at least present in a distant subarctic continental location. This modern isolate exhibits a nucleo-cytoplasmic replication cycle identical to that of *M. sibericum*. Its spherical particle (0.6-µm in diameter) encloses a 648-kb GC-rich double stranded DNA genome coding for 480 proteins of which 61 % are unique to these two molliviruses. The 461 homologous proteins are highly conserved (92 % identical residues in average) despite the presumed stasis of *M. sibericum* for the last 30,000 years. Selection pressure analyses show that most of these proteins contribute to the virus fitness. The comparison of these first two molliviruses clarify their evolutionary relationship with the pandoraviruses, supporting their provisional classification in a distinct family, the *Molliviridae*, pending the eventual discovery of intermediary missing links better demonstrating their common ancestry.

41

42 **Importance**

43 Virology has long been viewed through the prism of human, cattle or plant diseases leading to a
44 largely incomplete picture of the viral world. The serendipitous discovery of the first giant virus
45 visible under light microscopy (i.e., >0.3µm in diameter), mimivirus, opened a new era of virology,
46 now incorporating protozoan-infecting viruses. Planet-wide isolation studies and metagenomes
47 analyses have shown the presence of giant viruses in most terrestrial and aquatic environments
48 including upper Pleistocene frozen soils. Those systematic surveys have led authors to propose
49 several new distinct families, including the *Mimiviridae*, *Marseilleviridae*, *Faustoviridae*,
50 *Pandoraviridae*, and *Pithoviridae*. We now propose to introduce one additional family, the
51 *Molliviridae*, following the description of *M. kamchatka*, the first modern relative of *M. sibericum*,
52 previously isolated from 30,000-year old arctic permafrost.

53

Introduction

Studies started about 30 years ago, have provided multiple evidence that that soils frozen since the late Pleistocene and predominantly located in arctic and subarctic Siberia, do contain a wide diversity of microbes that can be revived upon thawing (1-3) after tens of thousands of years. These studies culminated by the regeneration of a plant from 30,000 year-old fruit tissue (4). Inspired by those studies, we then isolated from a similar sample two different Acanthamoeba-infecting large DNA viruses, named *Pithovirus sibericum* and *Mollivirus sibericum*, demonstrating the ability for these viruses, and maybe many others, to remain infectious after similarly long periods of stasis in permafrost (5-6). Several modern relatives to the prototype Pithovirus have since been isolated and characterized, leading to the emergence of the new proposed *Pithoviridae* family (7-10). In contrast, and despite the increasing sampling efforts deployed by several laboratories, no other relative of *M. sibericum* was found. Without additional isolates, it classification as a prototype of a new family, or as a distant relative of the pandoraviruses (with which it shared several morphological features and 16% of its gene content (6) remained an open question. Here we report the discovery and detailed characterization of the first modern *M. sibericum* relative, named *Mollivirus kamchatka*, after the location of the Kronotsky river bank where it was retrieved. The comparative analysis of these first two molliviruses highlights their evolutionary processes and suggests their provisional classification into their own family, the *Molliviridae*, distinct from the *Pandoraviridae*, pending the eventual discovery of intermediary missing links clearly establishing their common ancestry.

77 **Results**

78 **Virus isolation**

79 The original sample consisted of about 50 ml of vegetation-free superficial soil scooped (in sterile
80 tubes) from the bank of the Kronotsky river (coordinates: N 54°32'59'' E 160°34'55'') on july 6th,
81 2017. Before been stored at 4°C, the sample was transported in a backpack for a week at ambient
82 temperature (5° C up to 24° C). This area corresponds to a continental subarctic climate: very cold
83 winters, and short, cool to mild summers, low humidity and little precipitation. Back in the
84 laboratory, few grams of the sample were used in the Acanthamoeba co-cultivation procedure
85 previously described (6). After a succession of passages and enrichment on *Acanthamoeba*
86 *castellanii* cultures, viral particles were produced in sufficient quantity to be recovered and
87 purified.

88 **Virion morphology and ultrastructure**

89 As for *M. sibericum*, light microscopy of infected cultures showed the multiplication of particles.
90 Using transmission electron microscopy (TEM), these particles - undistinguishable from that of *M.*
91 *sibericum* - appear approximately spherical, 600 nm in diameter, lined by an internal lipid
92 membrane and enclosed in a 20 nm-thick electron-dense thick tegument covered with a mesh of
93 fibers (Fig. 1).

94 **Analysis of the replication cycle**

95 The replication cycle in *A. castellanii* cells was monitored using TEM and light microscopy of DAPI-
96 stained infected cultures as previously described (6). The suite of events previously described for
97 host cells infected by *M. sibericum*, was similarly observed upon *M. kamchatka* replication (6, 11).
98 After entering the amoeba cell through phagocytosis, *M. Kamchatka* virions are found gathered in
99 large vacuoles individually or in groups of 2-6 particles. Multiple nuclear events occur during the
100 infection starting with the drift of the host cell nucleolus to the periphery of the nucleus 4-5h post
101 infection (p.i.). 7h p.i., the nucleus appears filled with numerous fibrils that may correspond to viral

102 genomes tightly packed in DNA-protein complexes (Fig. 2A). About 30% of the nuclei observed at
103 that time exhibit a ruptured nuclear membrane (Fig. 2B). Besides those internal nuclear events, we
104 observed a loss of vacuolization within the host cell from 4h p.i. to the end of the cycle, in average
105 9h p.i. Large viral factories are formed in the cytoplasm at the periphery of the disorganized
106 nucleus (Fig. 2). These viral factories displays the same characteristics as those formed during *M.*
107 *sibericum* infections, involving an active recycling of membrane fragments (11).

108 **Comparative genomics**

109 DNA prepared from purified *M. kamchatka* particles was sequenced using both Illumina and
110 Oxford Nanopore platforms. *M. kamchatka* genome, a linear double stranded DNA molecule
111 (dsDNA), was readily assembled as a unique sequence of 648,864 bp. The read coverage was
112 uniform throughout the entire genome except for a 10 kb terminal segment presumably repeated
113 at both ends and exhibiting twice the average value. The *M. kamchatka* genome is thus
114 topologically identical to that of a *M. sibericum*, slightly larger in size (when including both terminal
115 repeats), and with the same global nucleotide composition (G+C= 60%). This similarity was
116 confirmed by the detailed comparison of their genome sequences exhibiting a global collinearity
117 solely interrupted by a few insertions and deletions.

118 Prior to the comparison of their gene contents, *M. sibericum* and *M. kamchatka* were both
119 annotated using the same stringent procedure that we previously developped to correct for gene
120 overpredictions suspected to occur in G+C rich sequences such as those of pandoraviruses (12-14).
121 A total of 495 and 480 genes were predicted for *M. sibericum* and *M. kamchatka*, with the
122 encoded proteins ranging from 51 to 2171 residues and from 57 to 2176 residues, respectively.
123 *M. kamchatka* predicted protein sequences were used in similarity search against the non-
124 redundant protein sequence database (15) and the re-annotated *M. sibericum* predicted
125 proteome. Out of the 480 proteins predicted to be encoded by *M. kamchatka* 463 had their closest
126 homologs in *M. sibericum*, with 92% identical residues in average. After clustering the paralogs,

127 these proteins corresponded to 434 distinct genes clusters delineating a first estimate of the
128 mollivirus core gene set. 411 of these clusters contained a single copy (singletons) gene for each
129 strain. Remarkably, 290 of the 480 (60.4 %) *M. kamchatka*-encoded proteins did not exhibit a
130 detectable homolog among cellular organisms or previously sequenced viruses (excluding *M.*
131 *sibericum*). Those will be referred to as "ORFans". Among the 190 proteins exhibiting significant
132 ($E<10^{-5}$) matches in addition to their *M. sibericum* counterparts, 78 (16%) were most similar to
133 Pandoravirus predicted proteins, 18 to proteins of other virus families (3.7%), 51 (10.6%) to *A.*
134 *castellanii* proteins, 24 (5%) to proteins of other eukaryotes, 17 (3.5%) to bacterial proteins and 2
135 (0.4%) to proteins of *Archaea* (Fig. 3).
136 The interpretation of these statistics are ambiguous as, on one hand, the large proportion of
137 "ORFans" (>60%) is characteristic of what is usually found for the prototypes of novel giant virus
138 families (7). On the other hand, the closest viral homologs are not scattered in diverse previously
139 defined virus families, but mostly belongs to the Pandoraviridae (78/96=81%) (Fig. 3). The two
140 molliviruses thus constitute a new group of viruses with their own specificity but with a
141 phylogenetic affinity with the pandoraviruses, as previously noticed (7). The proportion *M.*
142 *kamchatka* proteins with best matching counterparts in Acanthamoeba confirms the high gene
143 exchange propensity with the host, already noticed for *M. sibericum* (6).

144 **Recent evolutionary events since the *M. sibericum*/*M. kamchatka* divergence**

145 We investigated the evolutionary events specific of each of the molliviruses by focusing on proteins
146 lacking reciprocal best matches between the two strains. We found 63 such cases of which 10
147 corresponded to unilateral strain-specific duplications of genes, and 53 were unique to a given
148 strain. These unique genes (Table 1 & 2) result from gains or losses in either of mollivirus strains
149 (20 in *M. Kamchatka*, 33 in *M. sibericum*). The likely origins of these strain-specific genes
150 (horizontal acquisition, *de novo* creation (13, 14), or differential loss) are listed in Table 1 and Table
151 2.

152 Six *M. kamchatka* proteins, absent from *M. sibericum*, have homologs in pandoraviruses
153 suggesting common gene ancestors (and loss in *M. sibericum*) or horizontal acquisitions. According
154 to its embedded position within the pandoravirus phylogenetic tree, only one anonymous protein
155 (mk_165) could be interpreted as a probable horizontal transfer from pandoraviruses (Fig. 4A).
156 Another candidate, mk_92, shares 75% of identical residues with a pandoravirus DNA
157 methyltransferase (pqer_cds_559). However the very long branch associated to the P. dulcis
158 homolog (eventually due to a non-orthologous replacement) raises some doubt as for the origin of
159 the *M. kamchatka* gene (Fig. 4B).
160 Two *M. kamchatka*-specific proteins, encoded by adjacent genes (mk_466, mk_467), have
161 homologs in Acanthamoeba, suggesting potential host-virus exchanges. Phylogenetic
162 reconstruction did not suggested a direction for the transfer of mk_466. However, since the unique
163 homolog of mk_467 is found in Acanthamoeba (and not in other eukaryotes), the corresponding
164 gene probably originated from a close relative of *M. kamchatka* and was recently transferred to its
165 host.
166 Three proteins unique to *M. sibericum* have homologs in pandoraviruses, suggesting common
167 gene ancestors (and loss in *M. kamchatka*) or horizontal acquisitions. One protein (ms_14) has a
168 unique homolog in Acanthamoeba, suggesting a virus to host exchange. The homolog of ms_312 in
169 *Cavenderia fasciculata* (16) might be the testimony of past interactions between molliviruses and
170 deeply rooted ancestor of the Amoebozoa clade.
171 The above analyses of the genes unique to each mollivirus indicate that if horizontal transfer
172 may contribute to their presence, it is not the predominant mechanisms for their acquisition. We
173 then further investigated the 12 genes unique to *M. kamchatka* and 26 genes unique to *M.*
174 *sibericum* (i.e. “strain ORFans” w/o homolog in the databases) by computing three independent
175 sequence properties (Fig. 5): the codon adaptation usage index (CAI), the G+C composition, and
176 the ORF length.

177 With an average CAI value of 0.26, the strain-specific ORFans appear significantly different
178 from the rest of the mollivirus genes (mean = 0.40, Wilcoxon test $p < 2\ 10^{-7}$). These genes also
179 exhibit a significantly lower G+C content (56% for *M. kamchatka* and 57% for *M. sibericum*) than
180 the rest of the genes (60.5% for both viruses), also closer to the value computed for intergenic
181 regions (54% in average for both viruses). Moreover, the strain-specific ORFans are smaller in
182 average compared to the rest of the genes (115bp/378bp for *M. kamchatka* and 122bp/369bp for
183 *M. sibericum*). Altogether, those results suggests that *de novo* gene creation might occur in the
184 intergenic regions of molliviruses as already postulated for pandoraviruses (13, 14).

185 **New predicted protein functions in *M. kamchatka***

186 Sixty four of the *M. kamchatka* predicted proteins exhibit sequence motifs associated to known
187 functions. Fifty nine of them are orthologous to previously annotated genes in *M. sibericum* (6).
188 This common subset confirms the limited complement of DNA processing and repair enzymes
189 found in molliviruses (mainly a DNA polymerase: mk_287, a primase: mk_236, and 3 helicases:
190 mk_291, mk_293, mk_351), the absence of key deoxynucleotide synthesis pathways (such as
191 thymidylate synthase, thymidine kinase and thymidylate kinase), and of a ribonucleoside-
192 diphosphate reductase (present in pandoraviruses). The five *M. kamchatka* specific proteins (Table
193 1) associated to functional motifs or domain signature correspond to:
194 - two proteins (mk_93 and mk_104) containing a type of zinc finger (Ring domain) mediating
195 protein interactions,
196 - one protein (mk_469) with similarity to the (BI)-1 like family of small transmembrane proteins,
197 - one predicted LexA-related signal peptidase (mk_166),
198 - one DNA methyltransferase (mk_92).

199 **Evaluation of the selection pressure exerted on mollivirus genes**

200 The availability of two distinct strains of mollivirus allows the first estimation of the selection
201 pressure exerted on their shared genes during their evolution. This was done by the computation

202 of the ratio (ω=dN/dS) of the rate of non-synonymous mutations (dN) over the rate of synonymous
203 mutations (dS) for couples of orthologous genes. ω values much lesser than one are associated to
204 genes the mutation of which have the strongest negative impact on the virus fitness. The high
205 sequence similarity of proteins shared by *M. sibericum* and *M. kamchatka* allowed the generation
206 of flawless pairwise alignments and the computation of highly reliable ω values for most (i.e.
207 397/411) of their orthologous singletons.

208 Fourteen singleton pairs were not taken into account in the selection pressure analysis
209 because of their either identical or quasi-identical sequences (11 of them), or unreliable pairwise
210 alignments (3 of them). For the 397 gene pairs retained in the analysis, the mean ω value was 0.24
211 ± 0.14 (Fig. 6). This result corresponds to a strong negative selection pressure indicating that most
212 of the encoded proteins greatly contribute to the molliviruses' fitness. Together with the high level
213 of pairwise similarity (92%) of their proteins, this also indicates that *M. kamchatka* evolved very
214 little during the last 30,000 years and that the *M. sibericum* genome was not prominently damaged
215 during its cryostasis in permafrost.

216 The analysis restricted to the 244 pairs of ORFan-coding genes resulted in a very similar ω
217 value of 0.29± 0.15 (Fig. 6). This indicates that although homologs of these proteins are only found
218 in molliviruses, they have the same impact on the virus fitness than more ubiquitous proteins. This
219 confirms that they do encode actual proteins, albeit with unknown functions. In contrast, four
220 orthologous pairs (ms_160/mk_141; ms_280/mk_262; ms_171/ mk_151; ms_430/mk_411;
221 ms_60/mk_48) exhibit ω value larger than one. Those ORFans either are under positive selection
222 for maintaining their functions, or newly created gene products undergoing refinement or
223 pseudogenization.

224 We further examined the selection pressure of proteins-coding genes with homologs in
225 pandoraviruses. We used their 10 sequenced genomes to generate the corresponding gene
226 clusters (Fig. 7). The 90 clusters shared by both virus groups included 64 singletons (single copy

227 gene present in all viruses), among which 55 were suitable for dN/dS computations. The mean ω
228 value (0.17 ± 0.1) was very low, indicating that these genes, forming a "super core" gene set
229 common to the molliviruses and pandoraviruses, are under an even stronger negative selection
230 pressure than those constituting the provisional (most likely overestimated) mollivirus core gene
231 set .

232 **Genomic inhomogeneity**

233 The original genome analysis of Lausannevirus (a member of the Marseilleviridae family) (17)
234 revealed an unexpected non-uniform distribution of genes according to their annotation.
235 "Hypothetical" genes (i.e. mostly ORFans) were segregated from "annotated" (i.e. mostly non-
236 ORFans) in two different halves of the genome. In a more recent work, we noticed a similar bias in
237 the distribution of Pandoravirus core genes (13). The availability of a second mollivirus isolate gave
238 us the opportunity to investigate this puzzling feature for yet another group of Acantamoeba-
239 infecting virus. In Fig. 8, we plotted the distribution of three types of genes: 1- those with
240 homologs in *A. castellanii* (n= 55 for *M. sibericum* and n= 51 for *M. kamchatka*), 2- those belonging
241 to the super core set shared by both molliviruses and pandoraviruses (n=64), 3- those unique to
242 either mollivirus strains (n=26 for *M. sibericum*, n=12 for *M. kamchatka*). These plots reveal a
243 strong bias in the distribution of the super core vs. ORFan genes (Fig. 8). The first half of the *M.*
244 *sibericum* genome exhibits 90% of its ORFans while the second half contains most of the members
245 of the super core gene set. In contrast, genes eventually exchanged with the host display a more
246 uniform distribution. The lack of an apparent segregation in the distribution of ORFans in the *M.*
247 *kamchatka* genome might be due their underprediction as no transcriptome information is
248 available for this strain. Fig. 9 shows that there is also a strong bias in the distribution of single-
249 copy genes vs. those with paralogs in either *M. sibericum* and/or *M. kamchatka*. Altogether, these
250 analyses suggest that the two genome halves follow different evolutionary scenario, the first half

concentrating the genomic plasticity (de novo gene creation, gene duplication), the other half concentrating the most conserved, eventually essential, gene content.

Discussion

Following the discovery of their first representatives, each families of giant (e.g. Mimiviridae, Pithoviridae, Pandoraviridae) and large (e.g. Marseilleviridae) viruses infecting acanthamoeba have expanded steadily, suggesting they were relatively abundant and present in a large variety of environments. One noticeable exception has been the molliviruses, the prototype of which remained unique after its isolation from 30,000-year old permafrost. The absence of *M. sibericum* relatives from the large number of samples processed by us and others since 2014, raised the possibility that they might have gone extinct, or might be restricted to the Siberian arctic. Our isolation of a second representative of the proposed Molliviridae family, *M. kamtchatka*, at a location more than 1,500 km from the first isolate and enjoying a milder climate, is now refuting these hypotheses. Yet, the planet-wide ubiquity of these viruses remains to be established, in contrast to other acanthamoeba-infecting giant viruses (7). Even when present, mollivirus-like viruses appear to be in very low abundance, as judged from the very small fraction of metagenomics reads they represent in total sample DNA for *M. kamchatka* (about 0.02 part per million) as well as for *M. sibericum* (about one part per million)(6). Another possibility would be that the actual environmental host is not an acanthamoeba, the model host used in our laboratory. However, evidences of specific gene exchanges with acanthamoeba (including a highly conserved homolog major capsid protein) (6, 18, 19) make this explanation unlikely. We conclude that members of the proposed Molliviridae family are simply less abundant than other acanthamoeba-infecting viruses, a conclusion further supported by the paucity of Mollivirus-related sequences in the publicly available metagenomics data (data not shown).

275 As always the case, the characterization of a second representative of a new virus
276 representative opened new opportunities of analysis. Unfortunately, the closeness of *M.*
277 *kamchatka* with *M. sibericum* limited the amount of information that could be drawn from their
278 comparison. For instance, the number of genes shared by the two isolates is probably a large
279 overestimate of the "core" gene set characterizing the whole family. On the other hand, the
280 closeness of the two isolates allowed an accurate determination of the selection pressure
281 (ω=dN/dS) exerted on many genes, showing that most of them, including mollivirus ORFans,
282 encode actual proteins the sequence of which are under strong negative selection and thus
283 contribute to the virus fitness. Given the partial phylogenetic affinity (i.e. 90 shared genes clusters)
284 of the mollivirus with the pandoraviruses, we also assessed the selection pressure exerted on 55 of
285 these "super core" genes, and found them under even stronger negative selection (Fig. 7). This
286 suggests that this super core gene set might have been present in a common ancestor to both
287 proposed families.
288 If we postulate that *M. sibericum* underwent into a complete stasis when it became frozen in
289 permafrost while *M. kamchatka* remained in contact with living acanthamoeba, we could consider
290 the two viral genomes to be separated by at least 30,000 years of evolution (eventually more if
291 they are not in a direct ancestry relationship)(20). The high percentage of identical residues (92%)
292 in their proteins correspond to a low substitution rate of 1.7 10^{-6} amino acid change /position/year.
293 This is an overestimate since the two viruses probably started to diverge from each other longer
294 than 30,000-year ago. This value is nevertheless comparable with estimates computed for
295 poxviruses (21) given the uncertainty on the number of replicative cycles occurring per year. The
296 high level of sequence similarity of *M. kamchatka* with *M. sibericum* also indicates that the later
297 did not suffer much DNA damage during its frozen stasis, even in absence of detectable virus-
298 encoded DNA repair functions.

299 Horizontal gene transfers with the host were suggested by the fact that 51 proteins shared by
300 the two mollivirus strains exhibited a second best match in acanthamoeba. Because no homolog is
301 detected in other eukaryotes for most of them, these transfers probably occurred in the mollivirus-
302 to-host direction. The clearest case is that of a major capsid protein homolog (mk_314, ml_347)
303 sharing 64% Identical residues with a predicted acanthamoeba protein (locus: XP_004333827).
304 Two other genes encoding proteins that have also homologs in molliviruses flank the
305 corresponding host gene. However, the corresponding viral genes are not collinear in *M. sibericum*
306 or *M. kamchatka* and were probably transferred from a different, yet unknown mollivirus strain.
307 The presence of a 100% conserved major capsid protein homolog in the genome of *M. kamchatka*
308 and *M. sibericum* is itself puzzling. Such protein (with a double-jelly roll fold) is central to the
309 structure of icosahedral particles (22). Consistent with its detection in *M. sibericum* virions (6), its
310 conservation in *M. kamchatka*, suggests that it still plays a role in the formation of the spherical
311 mollivirus particles, while it has no homolog in the pandoraviruses. Inspired by previous
312 observations made on the unrelated Lausannevirus genome (17), we unveiled a marked
313 asymmetry in the distribution of different types of protein-coding genes in the Mollivirus genomes.
314 As shown in Fig. 8 the left half of the genome concentrates most of the genes coding for strain-
315 specific ORFans while the right half concentrates most of super core genes shared with
316 pandoraviruses. This asymmetry is even stronger for the multiple copy genes while single-copy
317 genes are uniformly distributed along the genome (Fig. 9). The molliviruses thus appear to confine
318 their genomic “creativity” (de novo creation and gene duplication) in one-half of their genome,
319 leaving the other half more stable. An asymmetry in the distribution of the core genes was
320 previously noticed in the pandoravirus genomes (13). Such features might be linked to the
321 mechanism of replication that is probably similar for the two virus families. Further studies are
322 needed to investigate this process. The asymmetrical genomic distribution of pandoravirus core
323 genes and mollivirus super core genes might be a testimony of their past common ancestry.

Despite their differences in morphology, as well as in virion and genome sizes, the comparative analysis of the prototype *M. sibericum* and of the new isolate *M. kamchatka* confirms their phylogenetic affinity with the Pandoraviruses (Fig. 3, Fig. 10). However, it remains unclear whether this is due to a truly ancestral relationship between them, or if it only the consequence of numerous past gene exchanges favored by use of the same cellular host. From the perspective of the sole DNA polymerase sequence, the two known molliviruses do cluster with the pandoraviruses, albeit at a much larger evolutionary distance than usually observed between members of the same virus family (Fig. 10). In absence of an objective threshold, and pending the characterization of eventual "missing links", we thus propose to classify *M. sibericum* and *M. kamchatka* as members of the proposed Molliviridae family, distinct from the Pandoraviridae.

Materials and Methods

Virus isolation

We isolated *M. kamchatka* from muddy grit collected near Kronotski Lake, Kamchatka (Russian Federation N :54 32 59, E :160 34 55). The sample was stored for twenty days in pure rice medium (23) at room temperature. An aliquot of the pelleted sample triggered an infected phenotype on a culture of *Acanthamoeba castellanii Neff* (ATCC30010TM) cells adapted to 2,5µg/mL of Amphotericin B (Fungizone), Ampicillin (100µg/ml), Chloramphrenicol (30µg/ml) and Kanamycin (25µg/ml) in protease-peptone–yeast-extract–glucose (PPYG) medium after two days of incubation at 32°C. A final volume of 6 mL of supernatant from two T25 flasks exhibiting infectious phenotypes was centrifuged for 1 hour at 16,000xg at room temperature. Two T75 flasks were seeded with 60,000 cells/cm² and infected with the resuspended viral pellet. Infected cells were cultured the same culture conditions as described below. We confirmed the presence of viral particles by light microscopy.

Validation of the presence of *M. kamchatka* in the original sample

349 To confirm the origin of the *M. kamchatka* isolate from the soil of the Kronotsky river bank,
350 DNA was extracted from the sample and sequenced on an Illumina platform, leading to
351 340,320,265 pair-ended reads (mean length 150bp). These metagenomics reads were then
352 mapped onto the genome sequence of *M. kamchatka*. Seven matching (100 % Identity) pair-ended
353 reads (hence 14 distinct reads) were detected, indicating the presence of virus particles in the
354 original sample, although at very low concentration. However, the very low probability of such
355 matches by chance ($p<10^{-63}$) together with the scattered distribution of these matches along the
356 viral genome, further demonstrate the presence of *M. kamchatka* in the original sample.
357

358 **Virus Cloning**

359 Fresh *A. castellanii* cells were seeded on a 12-well culture plate at a final concentration of
360 70,000cells/cm². Cell adherence was controlled under light microscopy after 45 minute and viral
361 particles were added to at a multiplicity of infection (MOI) around 50. After 1 h, the well was
362 washed 15 times with 3 mL of PPYG to remove any viral particle in suspension. Cells were then
363 recovered by gently scrapping the well, and a serial dilution was performed in the next three wells
364 by mixing 200µL of the previous well with 500µL of fresh medium. Drops of 0.5µL of the last
365 dilution were recovered and observed by light microscopy to confirm the presence of a unique *A.*
366 *castellanii* cell. The 0.5µL droplets were then distributed in each well of three 24-well culture plate.
367 Thousand uninfected A. castellanii cells in 500µL of PPYG were added to the wells seeded with a
368 single cell and incubated at 32°C until witnessing the evidence of a viral production from the
369 unique clone. The corresponding viral clones were recovered and amplified prior purification, DNA
370 extraction and cell cycle characterization by electron microscopy.

371 **Virus mass production and purification**

372 A total number of 40 T75 flasks were seeded with fresh *A. castellanii* cells at a final
373 concentration of 60,000 cells/cm². We controlled cell adherence using light microscopy after 45

374 minute and flasks were infected with a single clone of *M. kamchatka* at MOI=1. After 48h hours of
375 incubation at 32°C, we recovered cells exhibiting infectious phenotypes by gently scrapping the
376 flasks. We centrifuged for 10 min at 500×g to remove any cellular debris and viruses were pelleted
377 by a 1-hour centrifugation at 6,800xg. The viral pellet was then layered on a discontinuous cesium
378 chloride gradient (1,2g/cm²/ 1,3g/cm²/ 1,4g/cm²/ 1,5g/cm²) and centrifuged for 20h at 103,000xg.
379 The viral fraction produced a white disk, which was recovered and washed twice in PBS and stored
380 at 4 °C or −80 °C with 7,5% DMSO.
381
382 **Infectious cycle observations using TEM**
383 Twelve T25 flasks were seeded with a final concentration of 80,000 cells/cm² in PPYG medium
384 containing ATB. In order to get a synchronous infectious cycle eleven flasks were infected by freshly
385 produced *M. kamchatka* at substantial MOI=40. The *A. castellanii* infected flasks were fixed by
386 adding an equal volume of PBS buffer with 5 % glutaraldehyde at different time points after the
387 infection : 1h pi, 2h pi, 3h pi, 4h pi, 5h pi, 6h pi, 7h pi, 8h pi, 9h pi, 10h pi and 25h pi. After 45min of
388 fixation at room temperature, cells were scrapped and pelleted for 5min at 500xg. Then cells were
389 resuspended in 1ml of PBS buffer with 2,5 % glutaraldehyde and stored at 4°C. Each sample was
390 coated in 1mm³ of 2 % low melting agarose using Microvette® and embedded in Epon-812 resin.
391 Optimized osmium-thiocarbohydrazide-osmium (OTO) protocol was used for staining the samples:
392 1h fixation in PBS with 2 % osmium tetroxide and 1.5 % potassium ferrocyanide, 20 min in water
393 with 1 % thiocarbohydrazide, 30min in water with 2 % osmium tetroxide , over night incubation in
394 water with 1 % uranyl acetate and finally 30min in lead aspartate. Dehydration was made using an
395 increasing concentration of ethanol (50 %, 75 %, 85 %, 95 %, 100 %) and cold dry acetone. Samples
396 were progressively impregnated with an increasing mix of acetone and Epon-812 resin mixed with
397 DDSA 0,34v/v and NMA 0,68v/v (33 %, 50 %, 75 % and 100%). Final molding was made using a
398 hard Epon-812 mix with DDSA 0,34v/v NMA 0,68v/v and 0,031v/v of DMP30 accelerator and

399 hardened in the oven at 60°C for 5 days. Ultrathin sections (90nm thick) were observed using a FEI
400 Tecnai G2 operating at 200kV.

401 **DNA Extraction**

402 *M. kamchatka* genomic DNA was extracted from approximately 5 x 10^9 purified virus particles
403 using Purelink Genomic extraction mini kit according to the manufacturer's recommendation. Lysis
404 was performed with in a buffer provided with the kit and extra DTT at a final concentration of
405 1mM.

406 **Genome sequencing and assembly**

407 *M. kamchatka* genome was assembled using Spades (24) with a stringent K-mer parameter
408 using both various iteration steps (k = 21,41,61,81,99,127) and the --careful option to minimize
409 number of mismatches in the final contigs.

410 **Annotation of *Mollivirus sibericum* and *Mollivirus kamchatka***

411 A stringent gene annotation of *M. sibericum* was performed as previously described (13) using
412 RNA-seq transcriptomic data (6). Stranded RNA-seq reads were used to accurately annotate
413 protein-coding genes. Stringent gene annotation of *M. kamchatka* was performed w/o RNA seq
414 data but taking into account protein similarity with *M. sibericum*. Gene predictions were manually
415 curated using the web-based genomic annotation editing platform Web Apollo (25). Functional
416 annotations of protein-coding genes of both genomes were performed using a two-sided approach
417 as already previously described (13). Briefly, protein domains were searched with the CD-search
418 tool (26) and protein sequence searching based on the pairwise alignment of hidden Markov
419 models (HMM) was performed against the Uniclust30 database using HHblits tool (27). Gene
420 clustering was done using Orthofinder's default parameters (28) adding the "-M msa -oa" option.
421 Strict orthology between pairs of proteins was confirmed using best reciprocal blastp matches.

422 **Selection Pressure Analysis**

423 Ratios of non-synonymous (dN) over synonymous (dS) mutation rates for pairs of orthologous
424 genes were computed from MAFFT global alignment (29) using the PAML package and codeml with
425 the « model = 2 » (30). A strict filter was applyied to the dN/dS ratio: dN > 0, dS > 0, dS ≤ 2 and
426 dN/dS ≤ 10. The computation of the Codon Adaptation Index (CAI) of both Mollivirus was
427 performed using the cai tool from the Emboss package (31).

428 **Metagenome sequencing, assembly and annotation**

429 All metagenomic sample were sequenced with DNA-seq paired-end protocol on Illumina HiSeq
430 platform at Genoscope producing 16 datasets of 2x150bp read length. Raw reads quality was
431 evaluated with FASTQC (32). Identified contaminants were removed and remaining reads were
432 trimmed on the right end using 30 as quality threshold with BBTools (33). Assemblies of filtered
433 data sets were performed using MEGAHIT (34) with the following options: "--k-list 33,55,77,99,127
434 --min-contig-len 1000". All filtered reads were then mapped to the generated contigs using
435 Bowtie2 (35) with the "--very-sensitive" option.

436 **Availability of data**

437 The *M. kamtchatka* annotated genome sequence is freely available from the public through the
438 Genbank repository (URL://www.ncbi.nlm.nih.gov/genbank/) under accession number XXXXX.

439

440 **Acknowledgements**

441 We are deeply indebted to our volunteer collaborator Alexander Morawitz for collecting the
442 Kamchatka soil sample. E Christo-Foroux is the recipient of a DGA-MRIS scholarship (201760003).
443 This project has received funding from the European Research Council (ERC) under the European
444 Union's Horizon 2020 research and innovation program (grant agreement No 832601) and from
445 the FRM prize "Lucien Tartois" to C. Abergel. The funding bodies had no role in the design of the
446 study, analysis, and interpretation of data and in writing the manuscript.

447 **Competing interests**

The authors declare that they have no competing interests

450 **Figures**

451

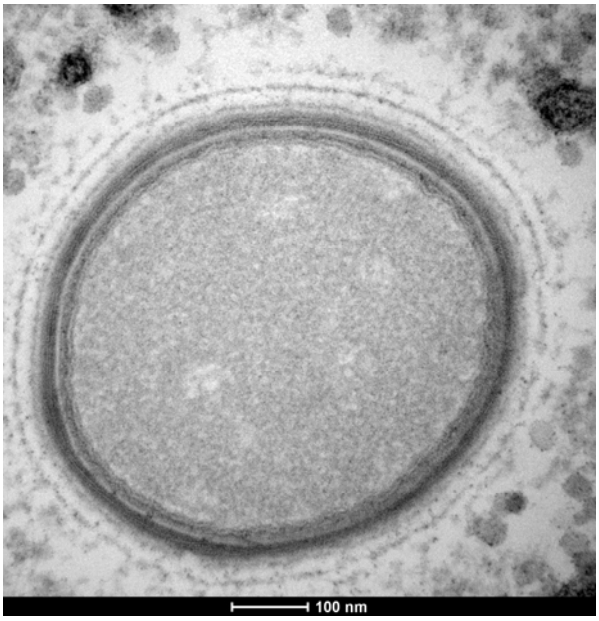

452

453 **Fig 1.** Ultrathin section TEM image of a neo-synthetized *M. kamchatka* particle in the cell

454 cytoplasm 7h post infection. The structures of the mature particle appears identical to that of *M.*

455 *sibericum.*

456

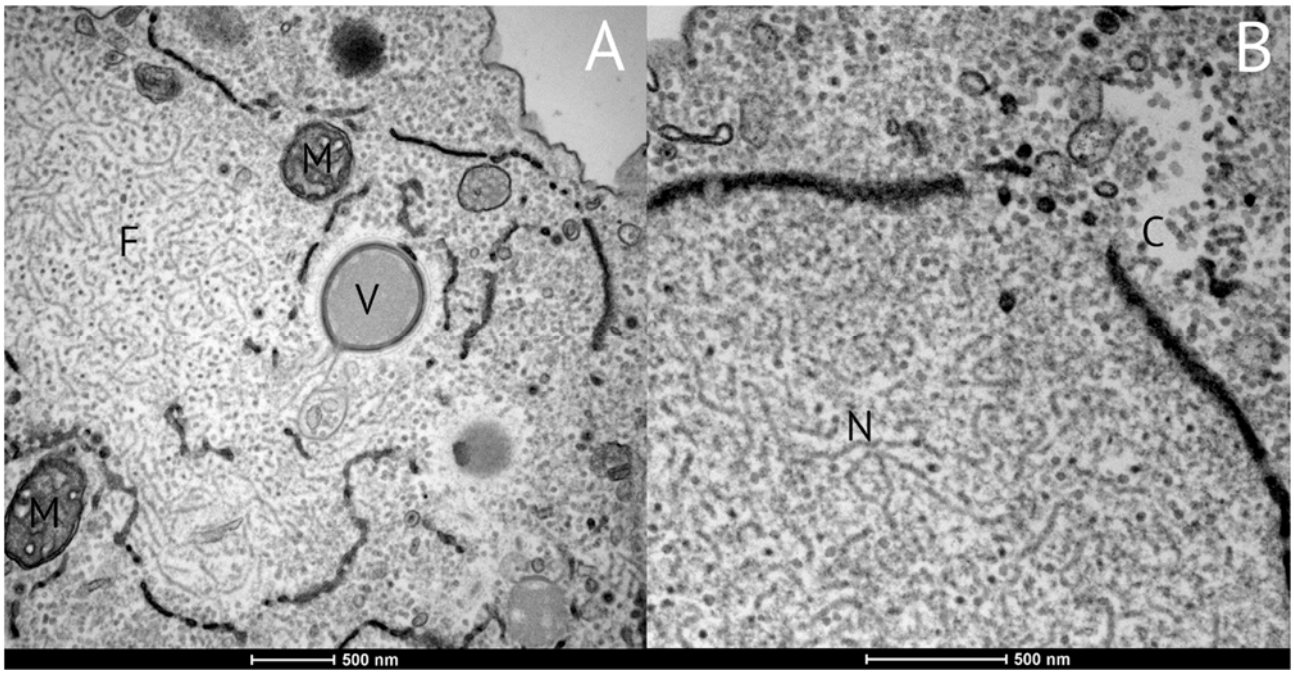

Fig 2. Ultrathin section TEM image of *A. castellanii* cell 7 to 10 hours post infection by *M. kamchatka*. (A) Viral factory exhibiting fibrils (F), a nascent viral particle (V), and surrounding mitochondria (M). Fragments of the ruptured nuclear membrane are visible as dark bead strings. (B) Details of a nuclear membrane rupture through which fibrils synthetized in the nucleus (N) are shed into the cytoplasm (C).

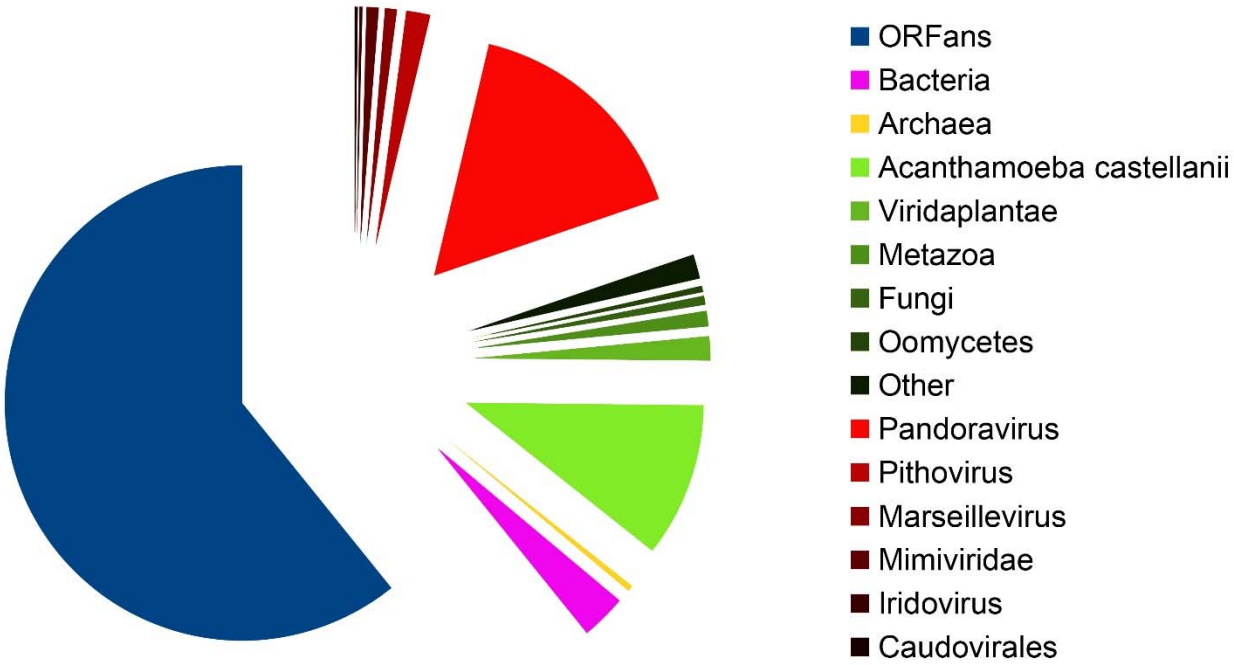

Fig 3. Distribution of the best-matching homologs to *M. kamchatka* predicted proteins. Best-matching homologous proteins were identified using BLASTP (E value $<10^{-5}$) against the non-redundant (NR) database (15) (after excluding *M. sibericum*). Green shades are used for eukaryotes, red shades for viruses.

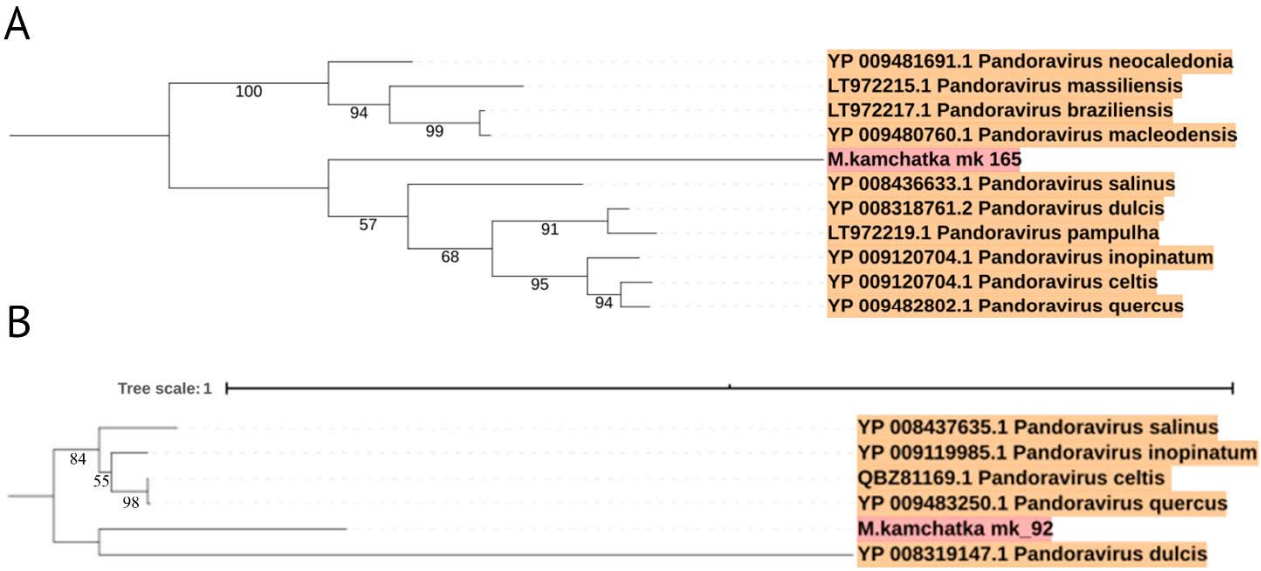

Fig 4. Eventual gene transfers from a pandoravirus to *M. kamchatka*. Both phylogenetic trees were computed from the global alignments of orthologous protein sequences using MAFFT (29). IQtree (36) was used to determine the optimal substitution model (options: « -m TEST » and « –bb 1000 »). (A) Protein mk_165 (no predicted function). (B) Predicted methyltransferase mk_92. Both *M. kamchatka* protein sequences appear embedded within the pandoravirus trees. In (A), the long branch leading to the *M. kamchatka* homolog suggests its accelerated divergence after an ancient acquisition from a pandoravirus. In (B), the long branch leading to the P. dulcis homolog might alternatively be interpreted as a non-orthologous replacement of the ancestral pandoravirus version of the gene.

485

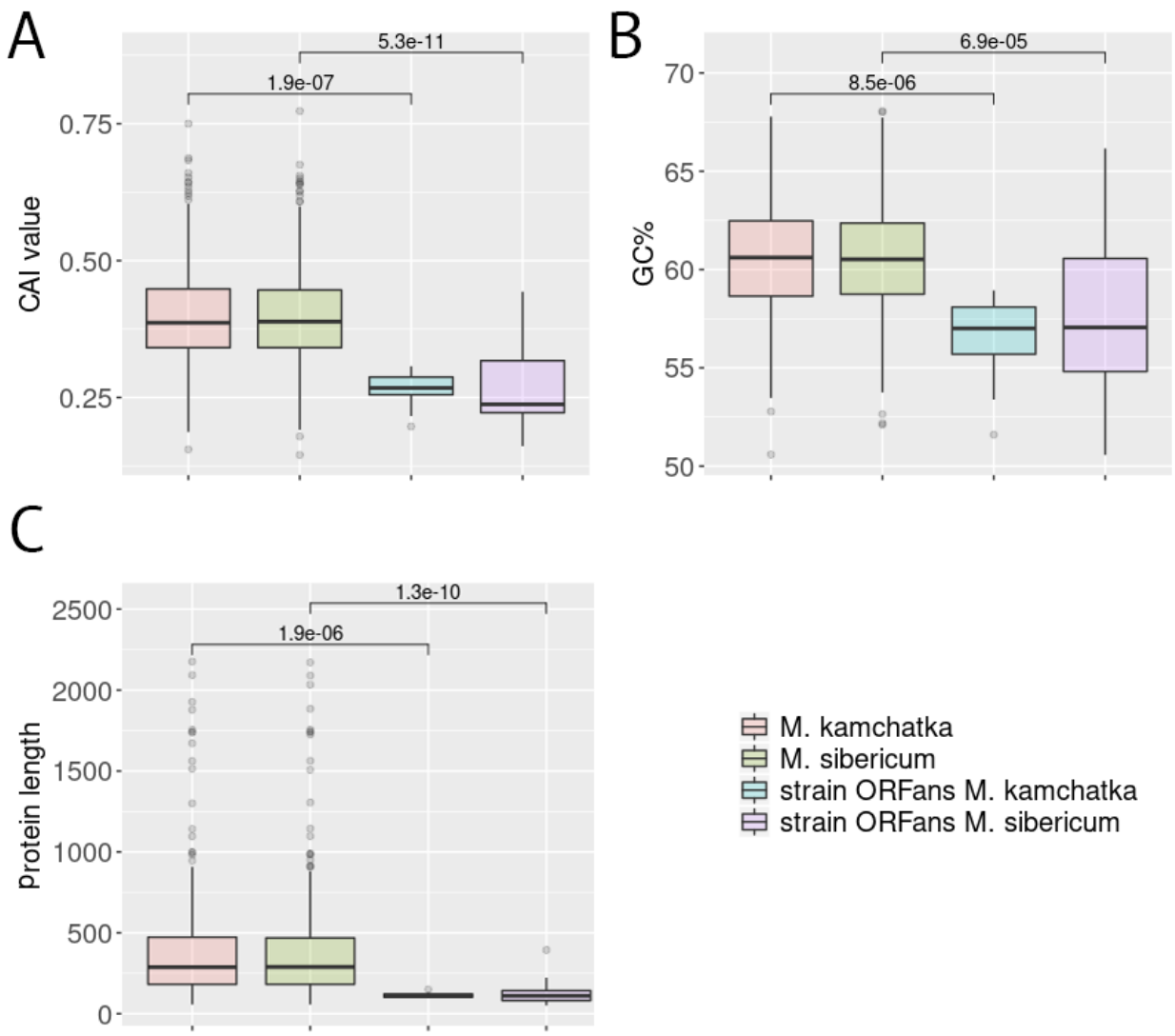

486

487

488 **Fig 5.** Genomic features of strain-specific ORFans. (A) Codon adaption index (CAI). (B) G+C content.

489 (C) Protein length. Box plots show the median, the 25th and 75th percentiles. P-value are

490 calculated using the Wilcoxon test.

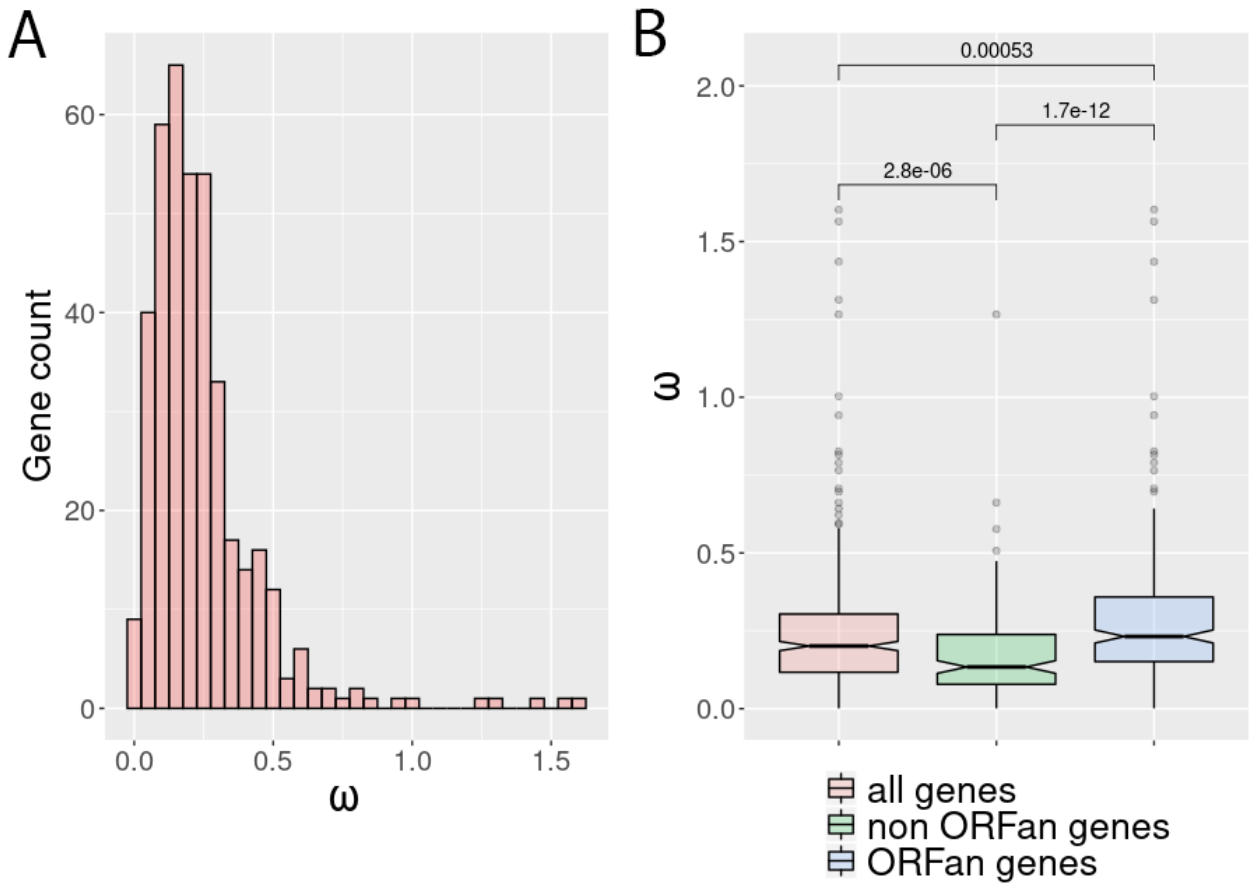

Fig 6. Selection pressure among different classes of genes. Values of ω (i.e. dN/dS) were computed from the alignments of homologous coding regions in *M. kamchatka* and *M. sibericum*. (A) Distribution of calculated ω values (n=397). (B) Box plots of the ω ratio among ORFan genes (n=243) and non ORFan genes (n=154). Box plots show the median, the 25th, and 75th percentiles. All p-value are calculated using the Wilcoxon test.

499

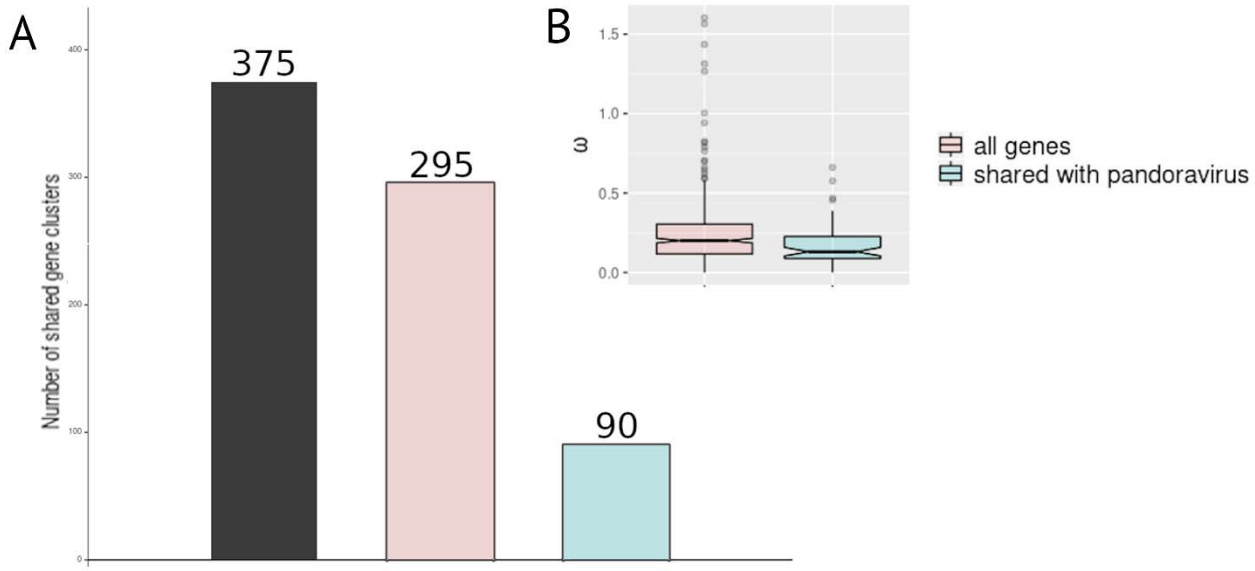

500

501 **Fig 7.** Comparison of the mollivirus and pandoravirus core gene contents. (A) The distribution of
502 the protein clusters shared by all pandoraviruses (black), the two Molliviruses (pink), and by both
503 virus groups (super core genes) (blue). (B) Box plot of ω values calculated from the alignment of
504 molliviruses core genes (pink), and super core genes (blue). Box plots show the median, the 25th,
505 and 75th percentiles.

506

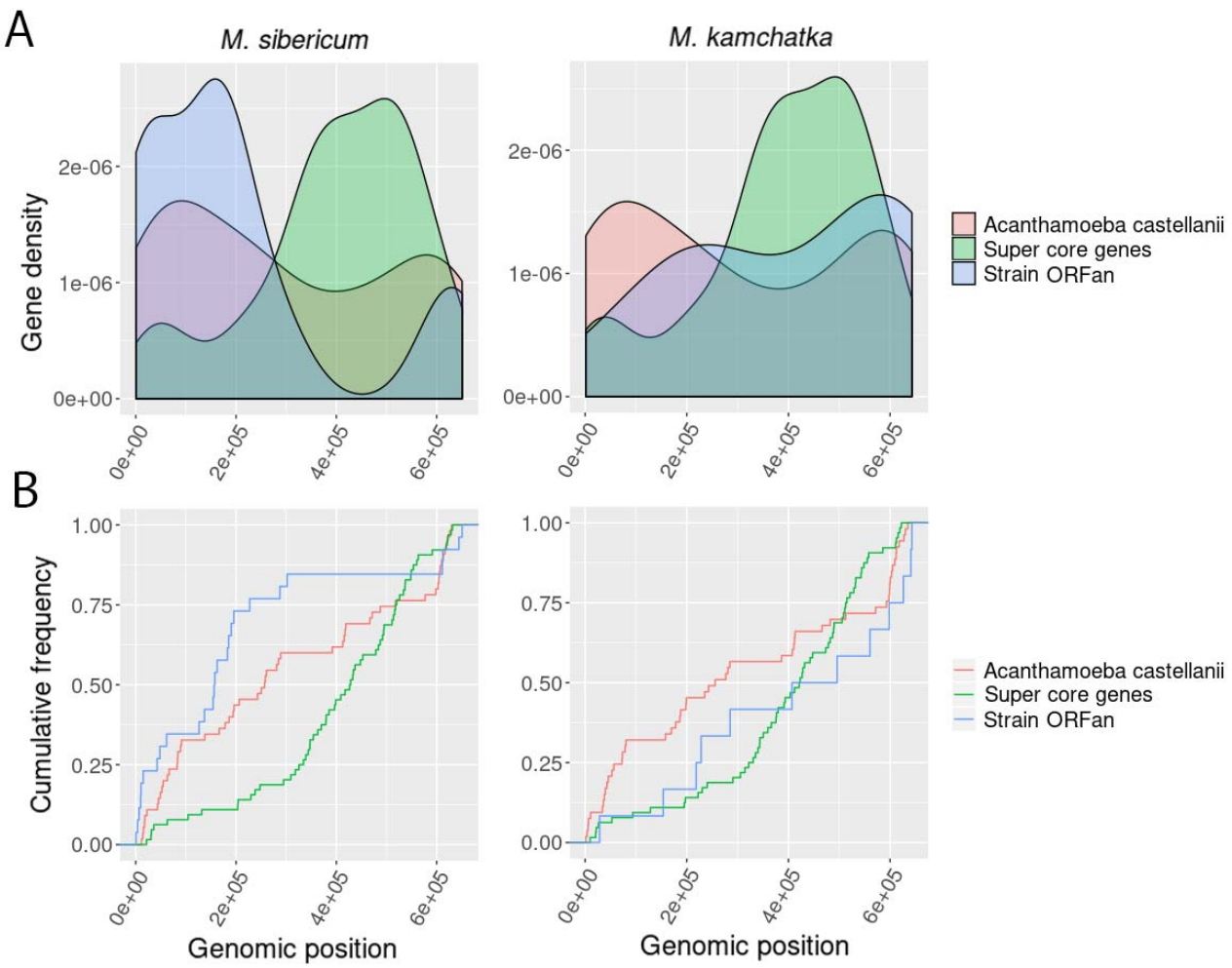

Fig 8. Distribution of different classes of genes along mollivirus genomes. (A) Variation of the gene density as computed by the ggplot2 “geom_density” function (37). Genes with best-matching homologs in *A. castellanii* (in the NR database excluding mollivirus) are uniformly distributed (in pink) in contrast to super core genes (in green) and strain-specific ORFans (in blue). (B) Cumulative distribution of the above classes of genes using the same color code.

515

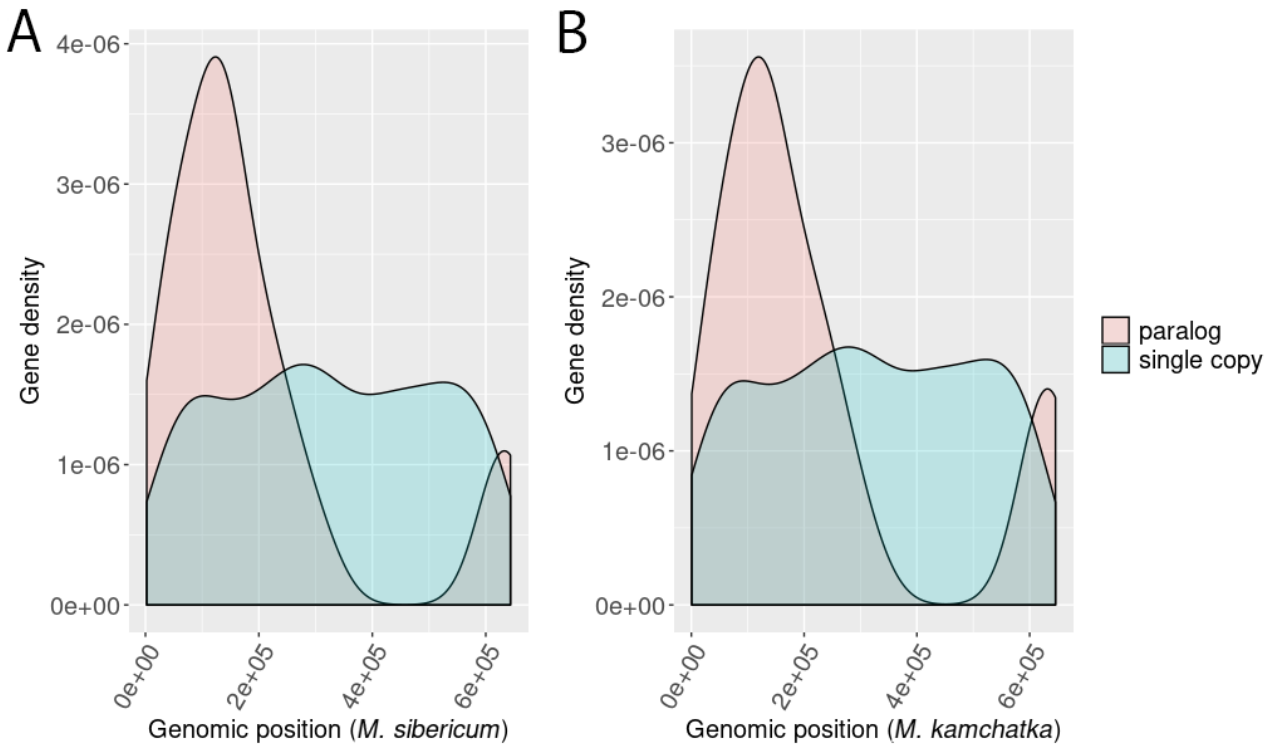

516

517 **Fig 9.** Distribution of single-copy *vs.* multiple copy genes along mollivirus genomes. Single copy

518 genes (in blue) in both strains are uniformly distributed in contrast to genes with paralogs (pink) in

519 at least one strain that cluster in the left half of the genomes. (A) *M. sibericum* (n=48). (B) *M.*

520 *kamchatka* (n= 46).

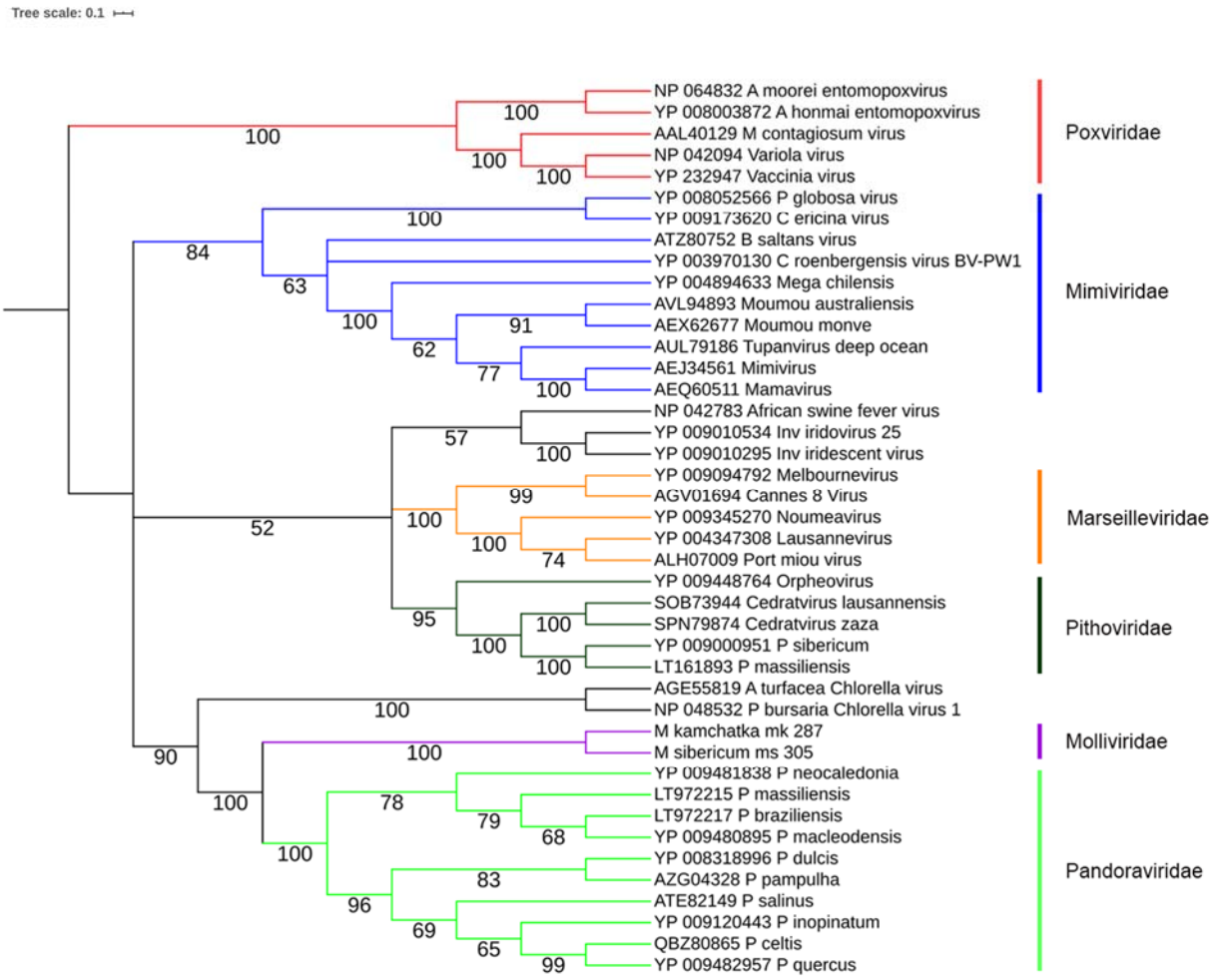

Fig 10. Phylogeny of DNA polymerase B of large and giant dsDNA viruses. This neighbor-joining tree was computed (JTT substitution model, 100 resampling) on 397 amino acid positions from an alignment of 42 sequences computed by MAFFT (29). Branches with boostrap values <60% were collapsed.

527 **Tables**

528

529 **Table 1.** Status of the protein-coding genes unique to *M. kamchatka*

ORF ID	Predicted function	Putative evolutionary scenario
mk_25	None (ORFan)	*de novo* creation or loss in *M. sibericum*
mk_92	DNA methyltransferase	loss in *M. sibericum* (present in some pandoraviruses)
mk_93	Ring domain	loss in *M. sibericum* (present in some pandoraviruses)
mk_104	Ring domain	loss in *M. sibericum* (present in some pandoraviruses)
mk_127	None (ORFan)	*de novo* creation or loss in *M. sibericum*
mk_159	None	loss in *M. sibericum* (present in some pandoraviruses)
mk_165	None	HGT from Pandoravirus
mk_166	Peptidase	loss in *M. sibericum* (present in some pandoraviruses)
mk_172	None (ORFan)	*de novo* creation or loss in *M. sibericum*
mk_182	None (ORFan)	*de novo* creation or loss in *M. sibericum*
mk_231	None (ORFan)	*de novo* creation or loss in *M. sibericum*
mk_313	None (ORFan)	*de novo* creation or loss in *M. sibericum*
mk_369	None (ORFan)	*de novo* creation or loss in *M. sibericum*
mk_415	None (ORFan)	*de novo* creation or loss in *M. sibericum*
mk_441	None (ORFan)	*de novo* creation or loss in *M. sibericum*
mk_466	None (ORFan)	*de novo* creation or loss in *M. sibericum*
mk_467	None	loss in *M. sibericum* (HGT to Acanthamoeba)
mk_469	B1-1 like	loss in *M. sibericum* (present in Acanthamoeba)
mk_476	None (ORFan)	*de novo* creation or loss in *M. sibericum*
mk_478	None (ORFan)	*de novo* creation or loss in *M. sibericum*

530

531 **Table 2.** Status of the protein-coding genes unique to *M. sibericum*

ORF ID	Predicted function	**Putative evolutionary scenario**
ms_1	None (ORFan)	De novo creation or loss in *M. kamchatka*
ms_3	None (ORFan)	De novo creation or loss in *M. kamchatka*
ms_5	None (ORFan)	De novo creation or loss in *M. kamchatka*
ms_7	None (ORFan)	De novo creation or loss in *M. kamchatka*
ms_8	None (ORFan)	De novo creation or loss in *M. kamchatka*
ms_13	None (ORFan)	De novo creation or loss in *M. kamchatka*
ms_14	None	HGT to Acanthamoeba
ms_38	None (ORFan)	De novo creation or loss in *M. kamchatka*
ms_42	None (ORFan)	De novo creation or loss in *M. kamchatka*
ms_53	None (ORFan)	De novo creation or loss in *M. kamchatka*
ms_64	None	loss in *M. Kamchatka* (present in Noumeavirus)
ms_109	None (ORFan)	De novo creation or loss in *M. kamchatka*
ms_120	None (ORFan)	De novo creation or loss in *M. kamchatka*
ms_136	None (ORFan)	De novo creation or loss in *M. kamchatka*
ms_138	None (ORFan)	De novo creation or loss in *M. kamchatka*
ms_139	None (ORFan)	De novo creation or loss in *M. kamchatka*
ms_144	None (ORFan)	De novo creation or loss in *M. kamchatka*
ms_157	None (ORFan)	De novo creation or loss in *M. kamchatka*
ms_159	None (ORFan)	De novo creation or loss in *M. kamchatka*
ms_166	None (ORFan)	De novo creation or loss in *M. kamchatka*
ms_172	None (ORFan)	De novo creation or loss in *M. kamchatka*
ms_190	None	loss in *M. kamchatka* (present in some pandoraviruses)
ms_193	None (ORFan)	De novo creation or loss in *M. kamchatka*
ms_246	None (ORFan)	De novo creation or loss in *M. kamchatka*
ms_258	None (ORFan)	De novo creation or loss in *M. kamchatka*
ms_311	Zinc-finger domain	loss in *M. kamchatka (*present in *Gossypium hirsutum)*
ms_312	Zinc-finger domain	loss in *M. kamchatka* (present in *Cavenderia fasciculata)*
ms_313	None	loss in *M. kamchatka* (present in some pandoraviruses)
ms_464	None (ORFan)	De novo creation or loss in *M. kamchatka*
ms_465	None (ORFan)	De novo creation or loss in *M. kamchatka*
ms_479	DNA methyltransferase	loss in *M. kamchatka* (present in some pandoraviruses)
ms_494	None (ORFan)	De novo creation or loss in *M. kamchatka*
ms_495	None (ORFan)	De novo creation or loss in *M. kamchatka*

532

533

534 **References**

535 1. Shi T, Reeves RH, Gilichinsky DA, Friedmann EI, 1997. Characterization of Viable Bacteria from
536 Siberian Permafrost by 16S rDNA Sequencing. Microb Ecol 33:169-179.
537 https://doi.org/10.1007/s002489900019.
538 2. Vishnivetskaya T, Kathariou S, McGrath J, Gilichinsky D, Tiedje JM 2000. Low-temperature
539 recovery strategies for the isolation of bacteria from ancient permafrost sediments. Extremophiles
540 4:165-173. https://doi.org/10.1007/s007920070031.
541 3. Graham DE, Wallenstein MD, Vishnivetskaya TA, Waldrop MP, Phelps TJ, Pfiffner SM, Onstott TC,
542 Whyte LG, Rivkina EM, Gilichinsky DA, Elias DA, Mackelprang R, VerBerkmoes NC, Hettich RL,
543 Wagner D, Wullschleger SD, Jansson JK. 2012. Microbes in thawing permafrost: the unknown
544 variable in the climate change equation. ISME J 6:709-712.
545 https://doi.org/10.1038/ismej.2011.163.
546 4. Yashina S, Gubin S, Maksimovich S, Yashina A, Gakhova E, Gilichinsky D. 2012. Regeneration of
547 whole fertile plants from 30,000-y-old fruit tissue buried in Siberian permafrost. Proc Natl Acad Sci
548 U S A 109:4008-4013. https://doi.org/10.1073/pnas.1118386109.
549 5. Legendre M, Bartoli J, Shmakova L, Jeudy S, Labadie K, Adrait A, Lescot M, Poirot O, Bertaux L,
550 Bruley C, Couté Y, Rivkina E, Abergel C, Claverie JM. 2014. Thirty-thousand-year-old distant relative
551 of giant icosahedral DNA viruses with a pandoravirus morphology. Proc Natl Acad Sci U S A
552 111:4274-4279. https://doi.org/ 10.1073/pnas.1320670111.
553 6. Legendre M, Lartigue A, Bertaux L, Jeudy S, Bartoli J, Lescot, M, Alempic JM, Ramus C, Bruley C,
554 Labadie K, Shmakova L, Rivkina E, Couté Y, Abergel C, Claverie JM. 2015. In-depth study of
555 Mollivirus sibericum, a new 30,000-y-old giant virus infecting Acanthamoeba. Proc Natl Acad Sci U
556 S A 112:E5327-E5335. https://doi.org/10.1073/pnas.1510795112.

557 7. Abergel C, Legendre M, Claverie JM. The rapidly expanding universe of giant viruses: Mimivirus,
558 Pandoravirus, Pithovirus and Mollivirus. 2015. FEMS Microbiol Rev 39:779-796.
559 https://doi.org/10.1093/femsre/fuv037.
560 8. Levasseur A, Andreani J, Delerce J, Bou Khalil J, Robert C, La Scola B, Raoult D. 2016. Comparison
561 of a Modern and Fossil Pithovirus Reveals Its Genetic Conservation and Evolution. Genome Biol
562 Evol 8:2333-2339. https://doi.org/10.1093/gbe/evw153.
563 9. Andreani J, Aherfi S, Bou Khalil JY, Di Pinto F, Bitam I, Raoult D, Colson P, La Scola B. 2016.
564 Cedratvirus, a Double-Cork Structured Giant Virus, is a Distant Relative of Pithoviruses. Viruses
565 8:300. https://doi.org/10.3390/v8110300.
566 10. Bertelli C, Mueller L, Thomas V, Pillonel T, Jacquier N, Greub G. 2017. Cedratvirus lausannensis -
567 digging into Pithoviridae diversity. Environ Microbiol 19:4022-4034.
568 https://doi.org/10.1111/1462-2920.13813.
569 11. Quemin ER, Corroyer-Dulmont S, Baskaran A, Penard E, Gazi AD, Christo-Foroux E, Walther P,
570 Abergel C, Krijnse-Locker J. 2019. Complex membrane remodeling during virion assembly of the
571 30,000-year-old Mollivirus sibericum. J Virol 93(13). pii: e00388-19.
572 https://doi.org/10.1128/JVI.00388-19.
573 12. Philippe N, Legendre M, Doutre G, Couté Y, Poirot O, Lescot M, Arslan D, Seltzer V, Bertaux L,
574 Bruley C, Garin J, Claverie JM, Abergel C. 2013. Pandoraviruses: amoeba viruses with genomes up
575 to 2.5 Mb reaching that of parasitic eukaryotes. Science 341:281-286.
576 https://doi.org/10.1126/science.1239181.
577 13. Legendre M, Fabre E, Poirot O, Jeudy S, Lartigue A, Alempic JM, Beucher L, Philippe N, Bertaux
578 L, Christo-Foroux E, Labadie K, Couté Y, Abergel C, Claverie JM. 2018. Diversity and evolution of the
579 emerging Pandoraviridae family. Nat Commun 9:2285.
580 https://doi.org/10.1038/s41467-018-04698-4.

581 14. Legendre M, Alempic JM, Philippe N, Lartigue A, Jeudy S, Poirot O, Ta NT, Nin S, Couté Y,
582 Abergel C, Claverie JM. 2019. Pandoravirus celtis illustrates the microevolution processes at work
583 in the giant Pandoraviridae genomes. Front Microbiol 10:430. https://doi.org/
584 10.3389/fmicb.2019.00430.
585 15. NCBI Resource Coordinators. 2018. Database resources of the National Center for
586 Biotechnology Information. Nucleic Acids Res 46:D8-D13. https://doi.org/10.1093/nar/gkx1095.
587 16. Heidel AJ, Lawal HM, Felder M, Schilde C, Helps NR, Tunggal B, Rivero F, John U, Schleicher M,
588 Eichinger L, Platzer M, Noegel AA, Schaap P, Glöckner G. 2011. Phylogeny-wide analysis of social
589 amoeba genomes highlights ancient origins for complex intercellular communication. Genome Res
590 21:1882-1891. https://doi.org/10.1101/gr.121137.111.
591 17. Thomas V, Bertelli C, Collyn F, Casson N, Telenti A, Goesmann A, Croxatto A, Greub G. 2011.
592 Lausannevirus, a giant amoebal virus encoding histone doublets. Environ Microbiol 13:1454-1466.
593 https://doi.org/10.1111/j.1462-2920.2011.02446.x.
594 18. Maumus F, Blanc G. 2016. Study of gene trafficking between acanthamoeba and giant viruses
595 suggests an undiscovered fof amoeba-infecting viruses. Genome Biol
596 Evol 8:3351-3363. https://doi.org/10.1093/gbe/evw260.
597 19. Chelkha N, Levasseur A, Pontarotti P, Raoult D, Scola B, Colson P. 2018. A phylogenomic study of
598 *Acanthamoeba polyphaga* draft genome sequences suggests genetic exchanges with giant viruses.
599 Front Microbiol 9:2098. https://doi.org/10.3389/fmicb.2018.02098.
600 20. Duchêne S, Holmes EC. 2018. Estimating evolutionary rates in giant viruses using
601 ancient genomes. Virus Evol 4:vey006. https://doi.org/10.1093/ve/vey006.
602 21. Hughes AL, Irausquin S, Friedman R. 2010. The evolutionary biology of poxviruses. Infect Genet
603 Evol 10:50-59. https://doi.org/10.1016/j.meegid.2009.10.001.
604 22. San Martín C, van Raaij MJ. 2018. The so far farthest reaches of the double jelly roll capsid
605 protein fold. Virol J 15:181. https://doi.org/10.1186/s12985-018-1097-1.

606 23. Arslan D, Legendre M, Seltzer V, Abergel C, Claverie JM. 2011. Distant Mimivirus relative with a
607 larger genome highlights the fundamental features of Megaviridae. Proc Natl Acad Sci U S A
608 108:17486-17491. https://doi.org/10.1073/pnas.1110889108.
609 24. Bankevich A, Nurk S, Antipov D, Gurevich A, Dvorkin M, Kulikov AS, Lesin V, Nikolenko S, Pham
610 S, Prjibelski A, Pyshkin A, Sirotkin A, Vyahhi N, Tesler G, Alekseyev MA, Pevzner P. 2012. SPAdes: A
611 New Genome Assembly Algorithm and Its Applications to Single-Cell Sequencing. J Comput Biol
612 19:455-477. https://doi.org/10.1089/cmb.2012.0021.
613 25. Dunn NA, Unni DR, Diesh C, Munoz-Torres M, Harris NL, Yao E, Rasche H, Holmes I, Elsik C,
614 Lewis S. 2019. Apollo: Democratizing genome annotation. PLoS Comput Biol 15: e1006790.
615 https://doi.org/10.1371/journal.pcbi.1006790.
616 26. Marchler-Bauer A, Derbyshire MK, Gonzales NR, Lu S, Chitsaz F, Geer LY, Geer RC, He J, Gwadz
617 M, Hurwitz DI, Lanczycki CJ, Lu F, Marchler GH, Song JS, Thanki N, Wang Z, Yamashita RA, Zhang D,
618 Zheng C, Bryant SH. 2015. CDD: NCBI's conserved domain database. Nucleic Acids Res 43:D222-
619 226. https://doi.org/10.1093/nar/gku1221.
620 27. Remmert M, Biegert A, Hauser A, Söding J. 2011. HHblits: lightning-fast iterative
621 protein sequence searching by HMM-HMM alignment. Nat Methods. 9:173-175.
622 https://doi.org/10.1038/nmeth.1818.
623 28. Emms DM, Kelly S. 2015. OrthoFinder: solving fundamental biases in whole genome
624 comparisons dramatically improves orthogroup inference accuracy. Genome Biol 16:157.
625 https://doi.org/10.1186/s13059-015-0721-2.
626 29. Katoh K, Misawa K, Kuma K-I, Miyata T. 2002. MAFFT: a novel method for rapid multiple
627 sequence alignment based on fast Fourier transform. Nucleic Acids Res 30:3059-3066.
628 https://doi.org/10.1093/nar/gkf436.
629 30. Yang Z. 2007. PAML 4: phylogenetic analysis by maximum likelihood. Mol Biol Evol 24:1586-
630 1591. https://doi.org/10.1093/molbev/msm088.

631 31 . Rice P, Longden I, Bleasby A. 2000. EMBOSS: the European molecular biology open software
632 suite. Trends Genet 16:276-277. https://doi.org/10.1016/s0168-9525(00)02024-2.
633 32. Andrews S. 2010. FastQC: a quality control tool for high throughput sequence data. Available
634 online at: http://www.bioinformatics.babraham.ac.uk/projects/fastqc .
635 33. Bushnell B, Rood J, Singer E. 2017. BBMerge – Accurate paired shotgun read merging via
636 overlap. PLoS ONE 12: e0185056. https://doi.org/10.1371/journal.pone.0185056.
637 34. Li D, Liu C-M, Luo R, Sadakane K, Lam T-W. 2015. MEGAHIT: An ultra-fast single-node solution
638 for large and complex metagenomics assembly via succinct de Bruijn graph. Bioinformatics
639 31:1674-1676. https://doi.org/10.1093/bioinformatics/btv033.
640 35. Langmead B, Salzberg SL. 2012. Fast gapped-read alignment with Bowtie 2. Nat Methods
641 9:357-359. https://doi.org/10.1038/nmeth.1923.
642 36. Nguyen LT, Schmidt HA, von Haeseler A, Minh BQ. 2015. IQ-TREE: A fast and effective stochastic
643 algorithm for estimating maximum likelihood phylogenies. Mol Biol Evol 32:268-274.
644 https://doi.org/10.1093/molbev/msu300.
645 37. Wickham H. ggplot2: Elegant Graphics for Data Analysis, p 33-74. 2016. Springer-Verlag New
646 York.